Received: 29 April 2020 | Revised: 12 August 2020 | Accepted: 16 August 2020

DOI: 10.1111/cas.14629

ORIGINAL ARTICLE

Cancer Science WILEY

Chaperone-mediated autophagy receptor modulates tumor growth and chemoresistance in non–small cell lung cancer

Akihiro Ichikawa[1] | Yu Fujita[1,2] | Yusuke Hosaka[1] | Tsukasa Kadota[1,2] | Akihiko Ito[1] | Shigehiro Yagishita[3] | Naoaki Watanabe[1,4] | Shota Fujimoto[1] | Hironori Kawamoto[1] | Nayuta Saito[1] | Masahiro Yoshida[1] | Mitsuo Hashimoto[1] | Shunsuke Minagawa[1] | Hiromichi Hara[1] | Noriko Motoi[5] | Yusuke Yamamoto[4] | Takahiro Ochiya[2,6] | Jun Araya[1] | Kazuyoshi Kuwano[1]

[1]Department of Internal Medicine, Division of Respiratory Diseases, The Jikei University School of Medicine, Tokyo, Japan

[2]Division of Molecular and Cellular Medicine, National Cancer Center Research Institute, Tokyo, Japan

[3]Division of Molecular Pharmacology, National Cancer Center Research Institute, Tokyo, Japan

[4]Division of Cellular Signaling, National Cancer Center Research Institute, Tokyo, Japan

[5]Department of Diagnostic Pathology, National Cancer Center Hospital, Tokyo, Japan

[6]Department of Molecular and Cellular Medicine, Institute of Medical Science, Tokyo Medical University, Tokyo, Japan

Correspondence
Yu Fujita, The Jikei University School of Medicine, Nishi-shimbashi 3-25-8, Minato-ku, Tokyo 105-8461, Japan.
Email: yuugot@jikei.ac.jp

Funding information
Japan Society for the Promotion of Science KAKENHI, Grant/Award Number: JP17K09672, JP17K09673, JP17K09674, JP18K08158, JP19K17649, JP19K08612 and JP19K08632; National Cancer Center Research and Development Fund, Japan

Abstract

Chaperone-mediated autophagy (CMA) is a lysosomal degradation pathway of selective soluble proteins. Lysosome-associated membrane protein type 2a (LAMP2A) is the key receptor protein of CMA; downregulation of LAMP2A leads to CMA blockade. Although CMA activation has been involved in cancer growth, CMA status and functions in non–small cell lung cancer (NSCLC) by focusing on the roles in regulating chemosensitivity remain to be clarified. In this study, we found that LAMP2A expression is elevated in NSCLC cell lines and patient's tumors, conferring poor survival and platinum resistance in NSCLC patients. LAMP2A knockdown in NSCLC cells suppressed cell proliferation and colony formation and increased the sensitivity to chemotherapeutic drugs in vitro. Furthermore, we found that intrinsic apoptosis signaling is the mechanism of cell death involved with CMA blockade. Remarkably, LAMP2A knockdown repressed tumorigenicity and sensitized the tumors to cisplatin treatment in NSCLC-bearing mice. Our discoveries suggest that LAMP2A is involved in the regulation of cancer malignant phenotypes and represents a promising new target against chemoresistant NSCLC.

KEYWORDS

apoptosis, chaperone-mediated autophagy, chemoresistance, LAMP2A, lung cancer

Ichikawa and Fujita equally contributed to this work.

1 | INTRODUCTION

Lung cancer is a leading cause of cancer-related death worldwide, and more than 85% of cases are classified as non–small cell lung cancer (NSCLC), including adenocarcinoma, squamous cell carcinoma, and large cell carcinoma.[1] Despite continuous development of chemotherapies including novel targeted therapies and cancer immunotherapies, the prognosis of lung cancer remains poor due to drug resistance and tumor recurrence. Further understanding of molecular mechanisms underlying the development of chemoresistance in NSCLC is an important issue for developing novel and effective therapeutic strategies.

Autophagy is the intracellular degradation system by which cytoplasmic materials are delivered to and degraded in the lysosome. It is subdivided into three subtypes: macroautophagy, microautophagy, and chaperone-mediated autophagy (CMA).[2] Macroautophagy delivers proteins and organelles to lysosomes for degradation upon sequestration in a double-membraned vesicle (autophagosome).[3] In microautophagy, the lysosome itself engulfs small components of the cytoplasm by inward invagination of the lysosomal membrane.[4] In contrast, protein substrates for CMA are selectively identified and targeted to the lysosomes through the interaction of a cytosolic chaperone protein HSC70. The substrate protein is taken up and degraded from lysosome-associated membrane protein type 2a (LAMP2A) on the lysosomal membrane, so the LAMP2A expression level reflects CMA activity.[5]

Currently, it has been reported that cancer cells upregulate their own CMA, a process that delivers selective cytosolic proteins to lysosomes for degradation, with pro-oncogenic effects.[6] Indeed, LAMP2A expression is elevated in many types of cancer, including gastric cancer, colon cancer, breast cancer, and NSCLC.[7] Selected proteins associated with cancer growth such as accumulated mutant p53 as well as misfolded nuclear receptor corepressor (NCOR) proteins have been shown to be degraded by CMA in cancer cells.[8,9] The bases for the pro-oncogenic effect of CMA are probably multiple and depend on the type and stage of cancer.[5,10] Although pathologic importance of LAMP2A expression reflecting CMA activity is well established in aging and neurodegenerative diseases,[5] a link between cancer malignancy and CMA remains to be fully identified.

In the present study, to learn more about the role of LAMP2A in cancer, we examined LAMP2A expression in tumor specimen from NSCLC patients and assessed clinical features such as cancer malignant phenotypes. Additionally, we also investigated whether LAMP2A affected cancer growth and drug resistance in vitro as well as in vivo. Our findings suggest that modulation of LAMP2A and, consequently, CMA represents a viable therapeutic target for chemoresistant NSCLC.

2 | MATERIALS AND METHODS

2.1 | Antibodies and reagents

Antibodies used were rabbit anti-LAMP2A (# ab125068; Abcam), mouse anti-β-actin (# A5316; Sigma-Aldrich), rabbit anti-caspase-3 (# 14220; Cell Signaling Technology), rabbit anti-Ki67 (# ab15580; Abcam), rabbit anti-p53 (# 9282; Cell Signaling Technology), rabbit anti-Bax (# 2870; Cell Signaling Technology), rabbit anti-Bcl-2 (# ab32503; Abcam), and rabbit anti-GAPDH (# 5174; Cell Signaling Technology). Cisplatin (CDDP) was obtained from Yakult Co., Ltd. Paclitaxel (PTX) was obtained from FUJIFILM Wako.

2.2 | Cell culture

Human NSCLC cell lines A549, H460, H226, PC9, PC14, and human bronchial epithelial cell line BEAS-2B were purchased from the American Type Culture Collection (ATCC). PC9CDDP and PC14CDDP[11] were kindly provided by Shien-Lab, Medical Oncology, National Cancer Center Hospital of Japan. These cells were maintained in RPMI 1640 medium (# 11875-093; Thermo Fisher Scientific) with 10% heat-inactivated fetal bovine serum and penicillin-streptomycin (# 15070-063; Thermo Fisher Scientific) at 37°C in 5% CO_2. The cumulative culture length of the cells was less than 6 months after resuscitation. Early-passage cells were used for all experiments and they were not reauthenticated.

2.3 | Lentiviral shRNA transduction

Cells were transfected with shRNAs using Lipofectamine 3000 (Invitrogen). The shRNAs (pLV-EGFP:T2A:Puro-U6) were purchased from VectorBuilder. shRNAs target human LAMP2A mRNA (target sequences of #1 5'-TCTAGTGTTGCTGGCTTATTT-3' and #2 5'-TGCCTTGGCAGGAGTACTTAT-3'). A random stuffer fragment (300 bp) from a noncoding sequence was inserted for proper negative control (NC) shRNA. Lentiviral particles were prepared using standard protocols. Briefly, shRNA plasmid and the second generation of packaging plasmids delta R8.2 and VSV-G (Addgene) were transfected into HEK293T cells (ATCC). Viral supernatants were collected after 48 hours of culture and used with polybrene (Sigma-Aldrich) for infection of indicated cell lines.

2.4 | siRNA transfection

NC siRNAs were purchased from Invitrogen (# AM4635). *LAMP2A* siRNA was designed by using BLOCK-iT™ RNAi Designer (https://rnaidesigner.thermofisher.com). The sequences of the regions targeted by the siRNA in the exon of the *LAMP2A* gene were 5'-GCAGTGCAGATGACGACAA-3 corresponding to bases 1230-1248. Transfections of indicated cell lines were performed using Lipofectamine3000.

2.5 | RNA extraction, reverse transcription, and quantitative real-time reverse transcription PCR (qRT-PCR)

Total RNA was extracted from cultured cells using QIAzol and the miRNeasy Mini Kit (Qiagen) according to the manufacturer's protocol.

The purity and concentration of all RNA samples were quantified using a NanoDrop ND-1000 spectrophotometer (Thermo Fisher Scientific). The reverse transcription reaction was performed using a High-Capacity cDNA Reverse Transcription Kit (Applied Biosystems) and a random hexamer primer. The synthesized cDNAs were quantified by SYBR Green I qRT-PCR. Quantitative real-time reverse transcription PCR (qRT-PCR) analysis was conducted using primers for human LAMP2A (forward: 5′-GCACAGTGAGCACAAATGAGT-3′; reverse: 5′-CAGTGGTGTGTATGGTGGGT-3′). β-actin (forward: 5′-CATGTACGTTGCTATCCAGGC-3′; reverse: 5′-CTCCTTAATGTCACGCACGAT-3′) was used for normalization of quantification. The relative amounts of LAMP2A were measured using the 2(-Delta Delta C(T)) method. The reactions were performed using an ABI 7300 Real-Time PCR System (Applied Biosystems). All reactions were performed in triplicate. Primer sequences were from Primer Bank (http://pga.mgh.harvard.edu/primerbank).

2.6 | Immunohistochemistry staining

Immunohistochemical (IHC) staining was performed as previously described with minor modification on the paraffin-embedded lung tissues.[12] Staining intensity of LAMP2A (# ab125068; Abcam) was scored using a four-tier scale from 0 (no staining) to 3 (strongest staining). Intensity scores were multiplied by the percentage of cancer cells with positive staining to generate an IHC score (maximum score, 300) by ImageJ, an open-source image processing program. Ki67 and caspase-3 IHC staining were assessed by measuring positively staining cells in the tumors at a magnification of X400 using ImageJ.

2.7 | Western blot analysis

Cultured cells were lysed in Mammalian Protein Extract Reagent (M-PER, # 78501; Thermo Fisher Scientific) with sample buffer solution (# 191-13272; FUJIFILM Wako). For each experiment, equal amounts of total protein were loaded onto 4%-20% SDS-PAGE. After SDS-PAGE, proteins were transferred to a polyvinylidene difluoride (PVDF) membrane (# ISEQ00010; Millipore). The membranes were incubated for 1 hour at room temperature with specific primary antibody including anti-LAMP2A (# ab125068; Abcam) was performed after blocking. After washing several times with Phsophate Buffered Saline with Tween 20, the membrane was incubated with anti-rabbit IgG, HRP-linked secondary antibody (# 7074; Cell Signaling Technology) or anti-mouse IgG, HRP-linked secondary antibody (# 7076; Cell Signaling Technology) followed by chemiluminescence detection (# 34080; Thermo Fisher Scientific, and # 1705061; BIO-RAD) with the ChemiDocTM Touch Imaging System (BIO-RAD).

2.8 | Cell viability assay

A Cell Counting Kit-8 (CCK-8; Dojindo) was used in the cell viability assay. A total of 3000 cells per well were seeded into 96-well plates. The cells were used for cell proliferation assays or cytotoxicity assays. For the cell proliferation assay, 10 μL of CCK-8 solution was added to each well after 24 hours, 48 hours, 72 hours, and 96 hours. The plate was further incubated for 2 hours at 37°C. The absorbance at 450 nm was measured. For cytotoxicity assays, the medium was aspirated off the following day and replaced with fresh media containing CDDP and PTX at different concentrations. After 3 days of culture, the plate was assayed by adding 10 μL of CCK-8 solution to each well, and the plate was further incubated for 2 hours at 37°C. The absorbance at 450 nm was measured. Cell viability is expressed as a percentage of the control cell viability. For each concentration of CDDP and PTX, the mean values of the mean absorbance rates from eight wells were calculated.

2.9 | Clonogenic assay

After harvesting with 0.05% trypsin, 200 cells were plated. Cells were incubated in 5% CO_2 atmosphere at 37°C for 14 days to allow colony formation. Colonies were fixed with methanol and stained with 1% crystal violet. The number of colonies with at least 50 cells was counted using ImageJ.

2.10 | Flow cytometry by annexin V-FITC conjugated with PI staining

Apoptosis was evaluated by flow cytometry, using annexin V-FITC and propidium iodide (PI) double staining following the manufacturer instruction of MEBCYTO apoptosis kit (MBL). Cells in each treated group were washed twice with cold PBS and then resuspended in binding buffer. A total of 1×10^6 cells/mL were transferred in a 5-mL tube containing 10 μL of annexin V-FITC and 5 μL of PI and were incubated for 15 minutes at room temperature in the dark. After adding 400 μL of binding buffer, the samples were analyzed by flow cytometry (Miltenyi Biotec MACSQuant) within 1 hour. Annexin V-positive cells were determined as apoptotic cells. Data analysis was performed with FlowJo software.

2.11 | Soft agar assay

Each 6-well plate was coated with 1.5 mL of bottom agar (RPMI 1640 containing 10% FBS and 0.5% Difco agar noble from BD Biosciences). Cells (5×10^3 cells) were suspended in 1.5 mL of top agar (RPMI 1640 containing 10% FBS and 0.35% Difco agar noble) into each well. Cells were cultured for approximately 2 weeks and replaced with fresh medium every 3 days. Colonies were stained using 0.005% crystal violet in 5% methanol and quantified using ImageJ software.

2.12 | Animal studies

The protocol of animal experiments was reviewed and approved by the Institutional Animal Care and Use Committee of the Jikei

University School of Medicine (No. 2018-052) and conformed to the Guidelines for the Proper Conduct of Animal Experiments of the Science Council of Japan (2006). Six- to seven-week-old male CB17.Cg-Prkdc^{scid}Lyst$^{bg\text{-}J}$/CrlCrlj mice (SCID-beige) or NOD/Shi-scid, IL-2RγKO Jic mice (NOG) (CLEA) were used in the experiments. The cells were resuspended in PBS as a half volume of inoculum and diluted with an equal volume of growth factor–reduced Matrigel (# 356 231; BD Biosciences). Lung cancer development was monitored twice a week for calculation of tumor volume. In the repeated administration study, the treatment (2.5 μg/kg of CDDP) was performed on days 34, 41, and 48 (once a week for 3 weeks, three treatments total).

2.13 | Clinical samples

The study protocol was approved by the Institutional Review Board at the National Cancer Center (Number: 2019-092). All materials were obtained with written informed consent and were provided by the National Cancer Center Biobank. All human lung tissue samples were derived from the resected lungs of lung cancer patients who had recurrence after pulmonary resection at the Department of Thoracic Surgery in the National Cancer Center Hospital between 1997 and 2010. According to the clinical database obtained from the Department of Thoracic Oncology Division in National Cancer Center Hospital, we selected 30 lung tumor samples with 12 corresponding normal lung tissues for LAMP2A expression analysis, and 36 lung tumor samples for LAMP2A expression analysis in the chemotherapeutic response of tumors for platinum-based chemotherapy (Tables S1 and S2). In this study, patients who were diagnosed with NSCLC (adenocarcinoma or squamous cell carcinoma) were enrolled. Upon removal of the surgical specimen, the research person immediately transported the tissues to the Biobank. Tissues were stored at − 80°C after snap freezing in liquid nitrogen. All tumors were reviewed by pathologists and were pathologically diagnosed according to the World Health Organization Classification of Tumors. The chemotherapeutic response of tumors for platinum-based chemotherapy was clinically evaluated according to the Response Evaluation Criteria in Solid Tumors (RECIST) as follows: (a) complete response, disappearance of all known disease; (b) partial response, 30% or more decrease in the entire tumor burden; (c) stable disease, less than 30% decrease or less than 20% increase in the entire tumor burden; and (d) progressive disease, 20% increase in the entire tumor burden or appearance of new lesions. In our report, subjects with complete response and partial response were defined as responders, and subjects with progressive disease were defined as nonresponders. Platinum-based chemotherapy was given for four or more cycles after recurrence. No cases received adjuvant chemotherapy after curative resection.[13]

2.14 | Statistics

The data presented in bar graphs are shown as the average (±SEM) for technical replicates. A Student *t*-test was used for comparison of two data sets. Analysis of variance (ANOVA) was used for multiple comparisons, followed by Tukey's or Dunnett's multiple comparison to find where the differences lie. Significance was defined as $P < 0.05$. Statistical software used was Prism version 8 (GraphPad Software, Inc).

3 | RESULTS

3.1 | High LAMP2A expression is associated with poor survival in NSCLC patients

To explore the role of CMA in NSCLC cells, we first verified the expression level of LAMP2A using qRT-PCR and Western blot analysis in various lung cancer cell lines (Figure 1A and B). In general, the LAMP2A proteins of lung cancer cell lines are highly glycosylated.[14,15] Although glycosylation might cause a discrepancy between mRNA and protein levels of LAMP2A, we found a higher expression of LAMP2A in A549, H460, H226, PC9, and PC14 cells than in normal human bronchial cells BEAS-2B. To investigate the roles of LAMP2A in NSCLC patients, we analyzed the protein expression level of LAMP2A in a cohort study of primary NSCLC tissues (30 cases) and adjacent normal lung tissues (12 cases) from patients with postoperative recurrence (Table S1). The IHC analysis revealed significantly higher LAMP2A expression in NSCLC patients who had recurrence after pulmonary resection compared with normal lung samples, and significant variation of LAMP2A expression, ranging from entirely negative to strongly positive, localized in the cytoplasm in NSCLC tumor samples (Figure 1C and D). The Kaplan-Meier analysis in the cohort study showed that the high expression levels of LAMP2A were significantly associated with poor relapse-free survival (Figure 1E). To further understand the potential biological significance

FIGURE 1 LAMP2A confers tumor survival in NSCLC patients. qRT-PCR analysis (A) and Western blot analysis (B) of the expression levels of LAMP2A in various lung cancer cell lines. $^{*}P < 0.05$, by ANOVA and Bonferroni's post-test. C, Immunohistochemical (IHC) staining for LAMP2A in representative normal lung tissues and tumors of lung cancer patients (negative & positive) (scale bar 100 μm). D, LAMP2A IHC score in normal lung tissue (n = 12) and tumor samples (n = 30). $^{***}P < 0.0001$, by Student's t-test. E, The relapse-free survival Kaplan-Meier curves were based on LAMP2A IHC score. A total of 30 tumor samples were divided into two groups based on LAMP2A IHC score. F, Relapse-free survival and overall survival Kaplan-Meier curves from GSE31210 using PrognoScan database (http://dna00.bio.kyutech.ac.jp/PrognoScan/index.html) were based on LAMP2A expression. NSCLC patients are stage I (n = 162) or stage II (n = 42). G, Enrichment plots of gene expression signatures for glycolysis, apoptosis, complement, mTORC1 signaling, hypoxia, and coagulation according to LAMP2A expression levels. The bar code plot indicates the positions of genes in each gene set; red and blue colors represent positive and negative Pearson correlations with LAMP2A expression, respectively

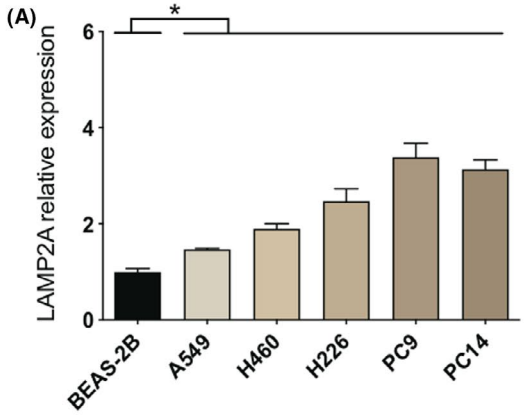
(A)
LAMP2A relative expression
6
4
2
0
*
BEAS-2B
A549
H460
H226
PC9
PC14

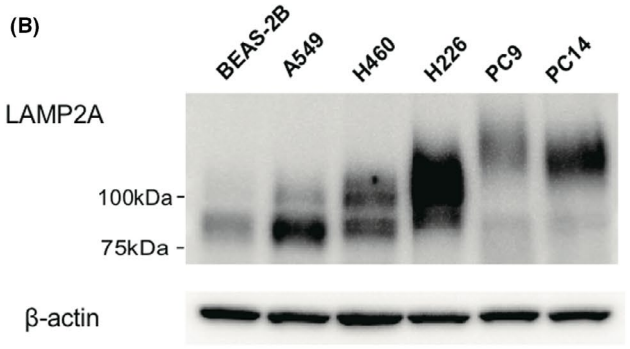
(B)
BEAS-2B
A549
H460
H226
PC9
PC14
LAMP2A
100kDa
75kDa
β-actin

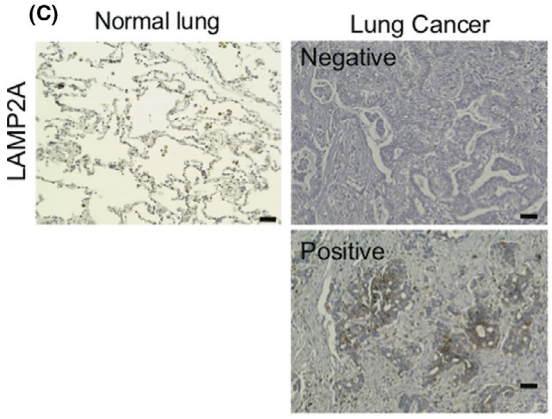
(C)
Normal lung
Lung Cancer
LAMP2A
Negative
Positive

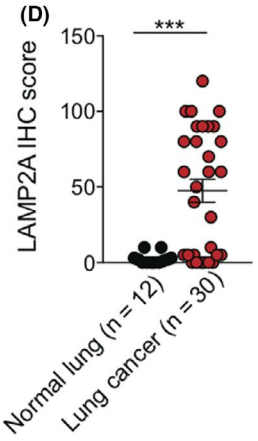
(D)
LAMP2A IHC score
150
100
50
0
***
Normal lung (n = 12)
Lung cancer (n = 30)

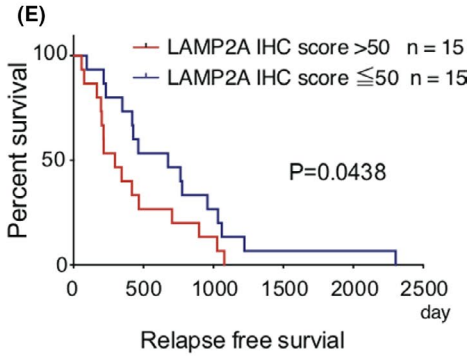
(E)
LAMP2A IHC score >50 n = 15
LAMP2A IHC score ≦50 n = 15
Percent survival
100
50
0
P=0.0438
0
500
1000
1500
2000
2500
day
Relapse free survial

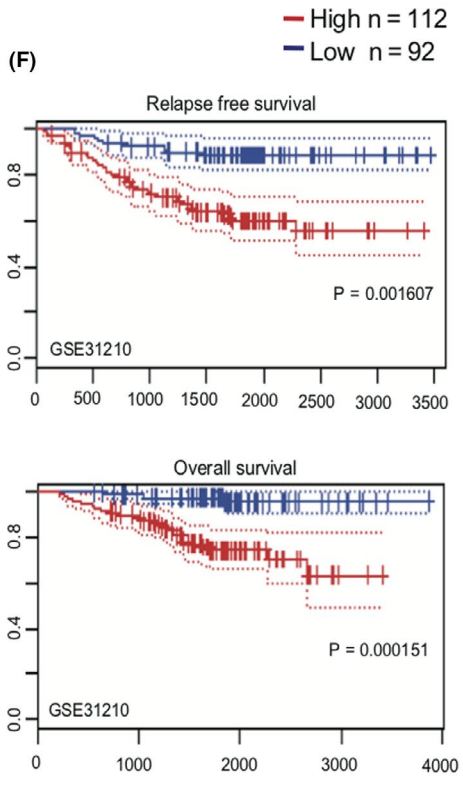
(F)
High n = 112
Low n = 92
Relapse free survival
P = 0.001607
GSE31210
0.8
0.4
0.0
0
500
1000
1500
2000
2500
3000
3500
Overall survival
P = 0.000151
GSE31210
0
1000
2000
3000
4000

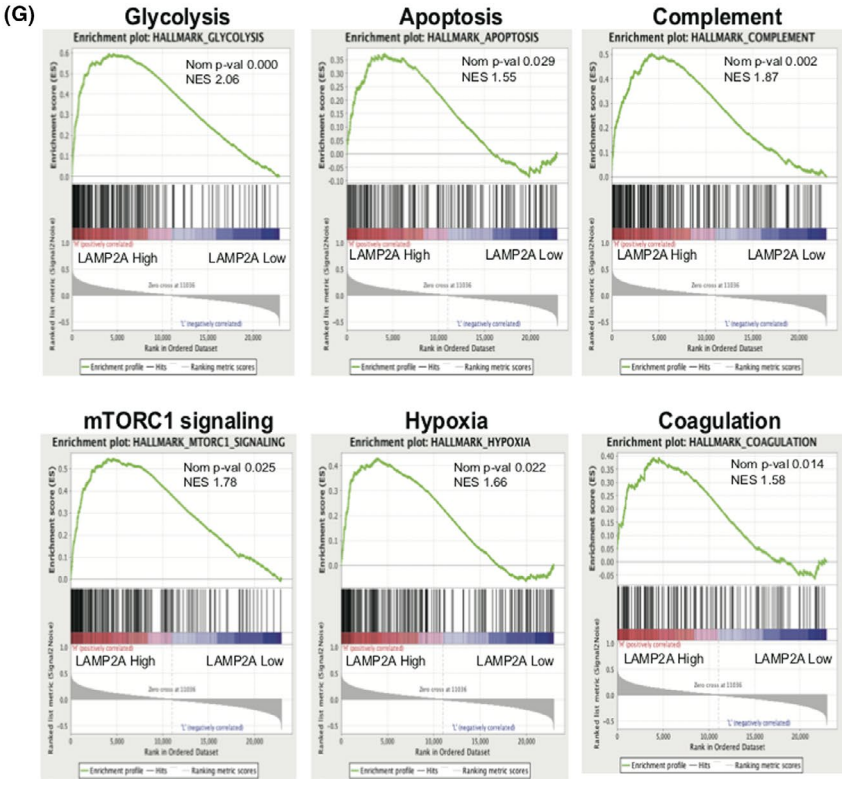
(G)
Glycolysis
Enrichment plot: HALLMARK_GLYCOLYSIS
Nom p-val 0.000
NES 2.06
Apoptosis
Enrichment plot: HALLMARK_APOPTOSIS
Nom p-val 0.029
NES 1.55
Complement
Enrichment plot: HALLMARK_COMPLEMENT
Nom p-val 0.002
NES 1.87
mTORC1 signaling
Enrichment plot: HALLMARK_MTORC1_SIGNALING
Nom p-val 0.025
NES 1.78
Hypoxia
Enrichment plot: HALLMARK_HYPOXIA
Nom p-val 0.022
NES 1.66
Coagulation
Enrichment plot: HALLMARK_COAGULATION
Nom p-val 0.014
NES 1.58
LAMP2A High
LAMP2A Low
Enrichment score (ES)
Ranked list metric (Signal2Noise)
Rank in Ordered Dataset

of a high LAMP2A expression level during lung cancer progression, we estimated the correlation between the LAMP2A expression profile and patient survival in the other cohort by using public database (Figure 1F). The Kaplan-Meier analysis from GSE31210[16] indicated that high expression levels of LAMP2A in early-stage NSCLC patients who had pulmonary resection were significantly associated with poor relapse-free survival ($P = 0.001607$) and overall survival ($P = 0.000151$). These findings suggest that a high LAMP2A expression level in NSCLC is associated with poor patient survival and may regulate lung cancer progression. To further examine the biological function and associated signal pathways that LAMP2A is possibly involved in, gene set enrichment analysis (GSEA) was performed using data from the cohort GSE 31 210. The GSEA results indicated that glycolysis, apoptosis, complement, mTORC1 signaling, hypoxia, and coagulation were evidently enriched in the LAMP2A-high group with a nominal *P*-value <0.05 and size > 100 (Figure 1G and Doc. S1). The data suggest that LAMP2A is involved in cancer-related signaling pathways, possibly resulting in poor survival in NSCLC.

3.2 | LAMP2A regulates lung cancer cell proliferation and chemoresistance through modulating intrinsic apoptosis signaling in vitro

In this study, we selected two NSCLC cell lines, A549 (mutant k-ras) and H460 (mutant PIK3CA) cells, in which to analyze the detailed function of LAMP2A in NSCLC. We conducted shRNA-based stable knockdown of LAMP2A in the two cell lines. The reduced expression of LAMP2A was verified by Western blot analysis (Figure 2A). The cell viability assay showed that LAMP2A shRNA significantly inhibited the cell proliferation of A549 and H460 cells (Figure 2B). We also performed clonogenic assay to determine the ability of LAMP2A to clonally expand and create colonies. Remarkably, knockdown of LAMP2A significantly decreased the colony number of A549 and H460 cells (Figure 2C and D). Next, we assessed the effects of LAMP2A knockdown on drug sensitivity. Notably, we observed that knockdown of LAMP2A in these cell lines sensitized the response of the cells to CDDP and PTX (Figure 2E). Furthermore, we found that expression levels of LAMP2A in drug-resistant cell line PC9/CDDP or PC14/CDDP were higher than those in their parental drug-sensitive PC9 or PC14, respectively (Figure 2F). To clarify the mode of cell death associated with reduced LAMP2A in lung cancer cells, we performed assay for apoptosis using flow cytometry in these cells after LAMP2A transient knockdown (Figure 2G). Annexin V staining revealed higher rates of apoptosis in A549 and H460 cells with LAMP2A transient knockdown. Further investigations with some key proteins in the intrinsic apoptosis pathway, such as p53, Bax, and Bcl-2 were performed with LAMP2A knockdown. In line with previous reports, the results showed that p53 and Bax expression increased and Bcl-2 expression decreased in H460 cells after LAMP2A transfection compared with NC shRNA transfection (Figure 2H and I). Along with decreased LAMP2A protein levels, glyceraldehyde 3-phosphate dehydrogenase (GAPDH), a representative selective target protein for CMA degradation,[17] was clearly increased, which may reflect decreased CMA activity (Figure 2H and I). Based on these data, LAMP2A can regulate malignant phenotypes of NSCLC in terms of apoptosis regulation through CMA modulation in vitro.

3.3 | LAMP2A knockdown contributes to the inhibition of tumorigenicity in vivo

For analyzing anchorage-independent growth as the function of LAMP2A, we used the soft agar colony formation assay to detect the malignant transformation in the lung cancer cells. In A549 and H460 cells, LAMP2A knockdown significantly formed fewer colonies in soft agar than the control cells (Figure 3A and B). Next, to validate the role of LAMP2A as a regulator of lung cancer progression in vivo, we examined the effects of LAMP2A knockdown on tumorigenicity using lung cancer xenograft models. Based on the data of tumor volume, LAMP2A knockdown in H460 cells inhibited tumorigenic ability 14 days after subcutaneous implantation compared with that in control cell-transplanted mice (Figure 3C and D). Furthermore, LAMP2A knockdown in H460 cells significantly reduced the cells with positive staining for Ki-67 and increased the cells with cleaved caspase-3 compared with the control group (Figure 3E and F). Collectively, these results showed that LAMP2A knockdown could significantly impede tumor growth in vivo.

3.4 | LAMP2A knockdown contributes to chemosensitivity in vivo

Next, to explore whether LAMP2A knockdown affected the chemoresistance of lung cancer cells to CDDP in vivo, tumors were

FIGURE 2 LAMP2A modulates lung cancer cell proliferation and chemoresistance in vitro. A, Western blot analysis of the expression levels of LAMP2A in A549 or H460 -shNC, -shLAMP2A#1, and #2 cells. B, Cell proliferation (%) of A549 or H460 -shNC, -shLAMP2A#1, and #2 cells. $^{**}P < .001$ and $^{***}P < .0001$, by ANOVA and Bonferroni's post-test. C, Representative images and (D) quantification of the colony number on clonogenic assay in A549 or H460 -shNC, -shLAMP2A#1, and #2 cells. $^{***}P < .0001$, by ANOVA and Bonferroni's post-test. E, Cell viability (%) was obtained by MTT with different doses of cisplatin (CDDP) or paclitaxel (PTX) in A549 or H460 -shNC, -shLAMP2A#1, and #2 cells. F, Western blot analysis of the expression levels of LAMP2A in PC9, PC9/CDDP, PC14, and PC14/CDDP cells. G, Apoptosis was detected by flowcytometric evaluation of FITC-Annexin V and PI double staining. Percentage of apoptosis was calculated by adding early apoptotic cells (Annexin V+/PI−) and late apoptotic/necrotic cells (Annexin V+/PI+). A549 or H460 cells were transfected with control or LAMP2A siRNA. Percentage of apoptotic cell count was assessed after 24 h treatment. $^{**}P < .001$, by Student's *t*-test. H, Western blot analysis and the quantifications (I) of the expression levels of LAMP2A, p53, Bax, Bcl-2, and GAPDH in H460 cells treated with shNC or shLAMP2A. $^{*}P < .05$, by Student's *t*-test

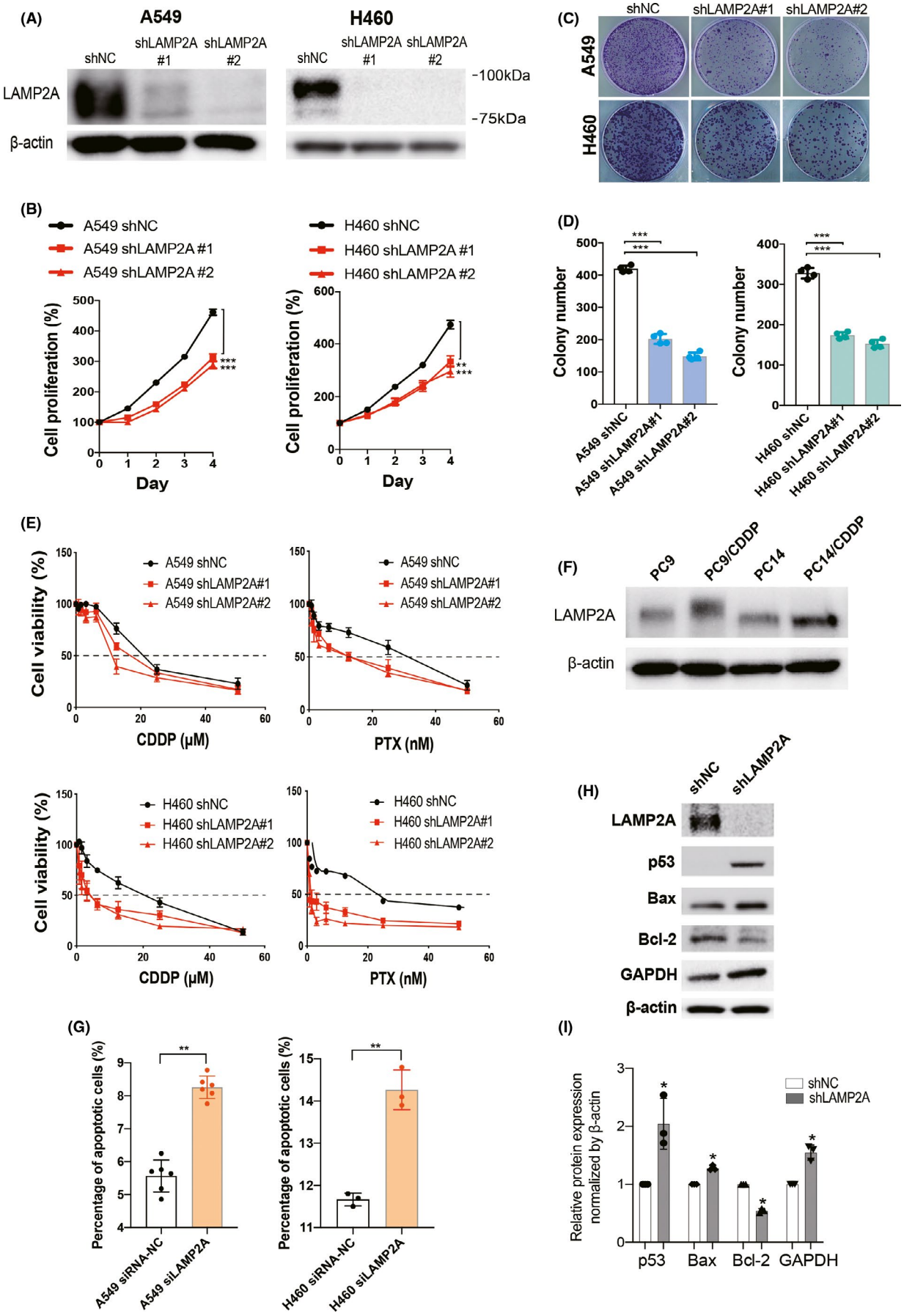
(A)
A549
H460
shNC
shLAMP2A #1
shLAMP2A #2
LAMP2A
β-actin
-100kDa
-75kDa
(B)
A549 shNC
A549 shLAMP2A #1
A549 shLAMP2A #2
H460 shNC
H460 shLAMP2A #1
H460 shLAMP2A #2
Cell proliferation (%)
Day
(C)
shNC
shLAMP2A#1
shLAMP2A#2
A549
H460
(D)
Colony number
A549 shNC
A549 shLAMP2A#1
A549 shLAMP2A#2
H460 shNC
H460 shLAMP2A#1
H460 shLAMP2A#2
(E)
Cell viability (%)
CDDP (μM)
PTX (nM)
(F)
PC9
PC9/CDDP
PC14
PC14/CDDP
LAMP2A
β-actin
(G)
Percentage of apoptotic cells (%)
A549 siRNA-NC
A549 siLAMP2A
H460 siRNA-NC
H460 siLAMP2A
(H)
shNC
shLAMP2A
LAMP2A
p53
Bax
Bcl-2
GAPDH
β-actin
(I)
Relative protein expression normalized by β-actin
shNC
shLAMP2A
p53
Bax
Bcl-2
GAPDH

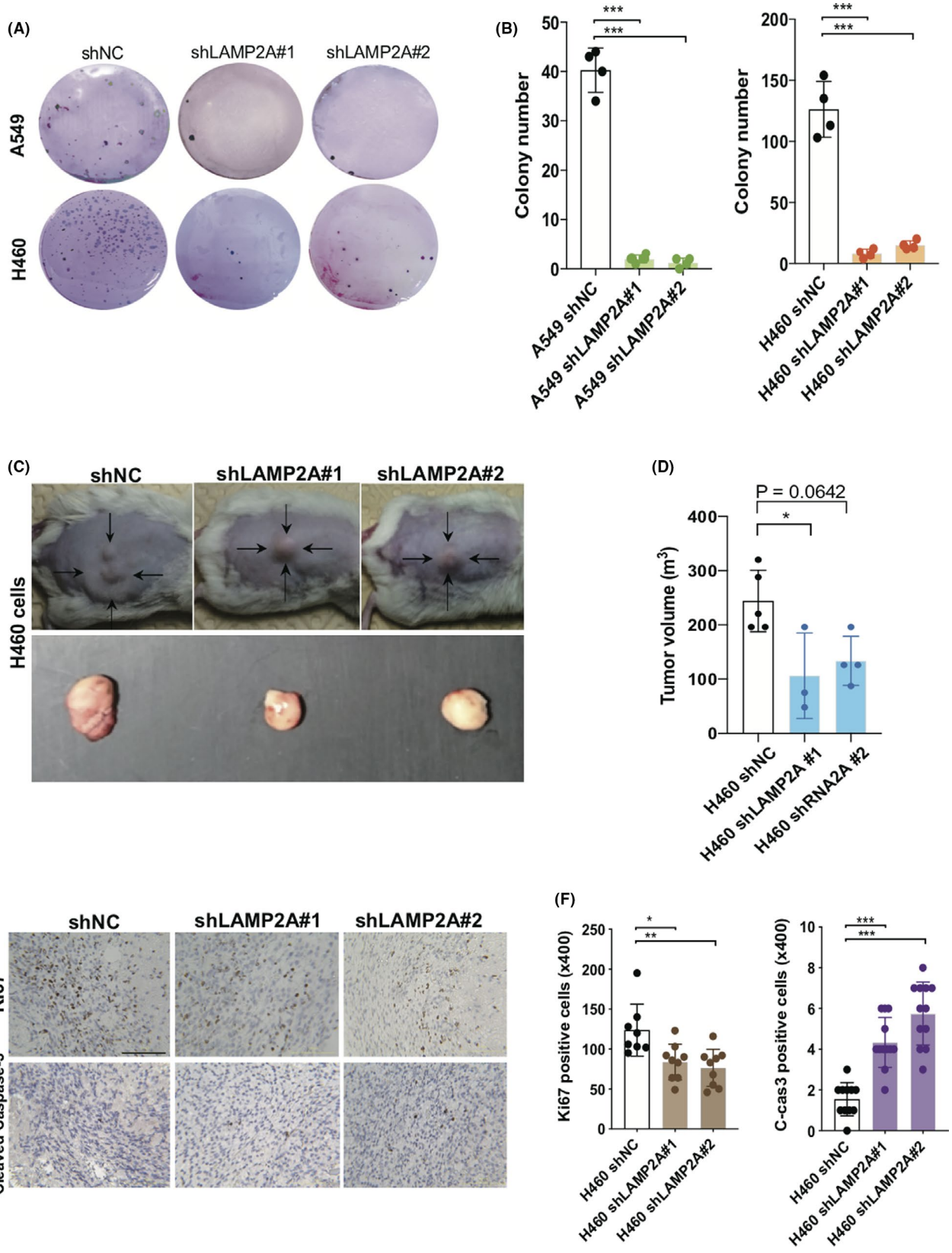

FIGURE 3 LAMP2A promotes anchorage-independent cancer cell growth and tumorigenicity in vivo. A, Representative images and (B) quantification of the colony number on soft agar colony formation in A549 or H460 -shNC, -shLAMP2A#1, and #2 cells. ***$P < .0001$, by ANOVA and Bonferroni's post-test. C, Representative pictures of subcutaneous tumors (indicated by arrows) and (D) tumor volume of H460 -shNC (n = 5), -shLAMP2A#1 (n = 3), and #2 cells (n = 4) at 14 days after subcutaneous implantation of $3x10^7$ cells into the SCID-beige mice. *$P < .05$, by ANOVA and Bonferroni's post-test. E and F, Immunohistochemical (IHC) staining for (E) Ki67 and (F) cleaved caspase-3 in the tumors of H460 -shNC, -shLAMP2A#1, and #2 cells (scale bar 100 μm). *$P < .05$, **$P < .01$ ***$P < .0001$, by ANOVA and Bonferroni's post-test

initiated in immunodeficient mice and then followed by an intraperitoneal injection of 2.5 mg/kg CDDP or the same amount normal saline (NS) once a week for 4 weeks (Figure 4A). At the point of starting CDDP treatment on day 34, there was no statistically significant difference in the tumor sizes between the four groups. At 8 weeks after subcutaneous implantation, the tumors formed in the H460-shLAMP2A–bearing mice were significantly smaller compared with the tumors in the H460-shNC–bearing mice after CDDP treatment (Figure 4B-D). Furthermore, we found that the cells with cleaved caspase-3 in the tumors formed in the H460-shLAMP2A–bearing mice with NS significantly increased compared with the tumors formed in the H460-shNC–bearing mice with CDDP treatment. On the other hand, we found that the tumors formed in the H460-shNC–bearing mice with CDDP treatment significantly reduced the cells with cyclin D1 compared with the tumors formed in the H460-shLAMP2A–bearing mice with NS (Figure 4E and F). Mechanistically, we speculated that CDDP treatment suppressed tumor cell cycle and LAMP2A knockdown induced tumor cell apoptosis, resulting in dramatic tumor reduction in the combination treatment. These results indicate that CMA blockade confers CDDP therapeutic advantages to lung cancer cells in vivo. To further examine whether LAMP2A is related with chemoresistance in NSCLC patients, we compared the LAMP2A expression in the responder (n = 19) with that in the nonresponder group (n = 17) to platinum-based chemotherapy (Table S2). In this cohort study, we observed increased LAMP2A expression in the tumors of the nonresponder group compared with that in the tumors of the responder group (Figure 4E). Furthermore, both univariate and multivariate analysis revealed that LAMP2A IHC score is a significant predictive factor for the response of platinum-based chemotherapy (Table S3).

Taken together, these data indicated that LAMP2A plays a pivotal role in cancer progression and chemoresistance, and demonstrate the clinical importance of the CMA-regulated pathway with LAMP2A modulation in NSCLC.

4 | DISCUSSION

Our preclinical data demonstrate the clinical relevance of CMA-mediated cancer malignancy and represents a promising novel target for LAMP2A against NSCLC. We showed that LAMP2A expression, a surrogate for CMA activity in human tumors, correlated with the response of NSCLC patients to platinum-based chemotherapy, suggesting this protein could be used as a valuable biomarker of the response. We also showed that LAMP2A may regulate antiapoptotic intrinsic signaling which, in turn, affected cancer malignant phenotypes and response to CDDP. Our data suggest that combination CMA blockade with platinum-based chemotherapy could have better therapeutic potential for NSCLC treatment.

CMA is a highly selective form of autophagy that targets cytosolic proteins carrying the KFERQ pentapeptide, a sequence found in approximately 30% of cytosolic proteins.[18] CMA plays a critical role in cellular quality control under physiological and pathological conditions. In terms of cancer biology, the first report by Kon et al showed that CMA is required for cancer cell proliferation in vitro because it contributes to the maintenance of the metabolic alterations characteristic of malignant cells.[6] Recently it has been shown that levels of LAMP2A expression, a surrogate for CMA activity in human tumors, are elevated in many tumors, including gastric cancer, colon cancer, breast cancer, and NSCLC.[7] It has been reported that blockade of CMA reduces their tumorigenic capabilities. Cancer cells depend on CMA for a variety of pro-oncogenic functions such as sustained glycolytic activity, resistance to stressors, and maintenance of high oncogene load.[10] Moreover, CMA confers resistance to cancer treatment through cell type–specific mechanisms. For instance, CMA prevents apoptosis and contributes to resistance to oxaliplatin in hepatocellular carcinoma by degrading the apoptosis trigger cyclin D1,[19] and to irradiation by degrading HMGB1.[20] Furthermore, active degradation of the acetyltransferase p300/CBP by CMA confers resistance to 5-fluorouracil in colorectal cancer.[21] However, it is still unclear how CMA is involved in chemosensitivity in NSCLC. Here, we speculate that LAMP2A modulates the response to platinum-based chemotherapy by modulating antiapoptotic intrinsic signaling in NSCLC patients.

For the treatment of NSCLC, patients who have genetic alterations in the epidermal growth factor receptor (EGFR), anaplastic lymphoma kinase (ALK), and ROS1 proto-oncogene receptor tyrosine kinase benefit from targeted therapies in the first-line setting and in subsequent lines. In patients with no known driver mutations or with wild-type tumors, immunotherapy with checkpoint inhibitors combined with platinum-based chemotherapy has revolutionized treatment. Although platinum-based chemotherapy is still used as first-line or second-line therapy for advanced lung cancer, there is no putative indicator which can predict whether the NSCLC patient would be chemoresistant or sensitive to the treatment. Therefore, elucidating the underlying mechanistic insights of CDDP resistance will be beneficial for improving the efficiency of chemotherapy as well as for developing novel therapeutic strategies to decrease recurrence and to improve NSCLC patient survival. Based on our data, the underlying mechanisms by CMA in NSCLC may allow stratification of treatment selection based on LAMP2A expression levels as well as developing molecular targeting to improve the efficacy of platinum-based chemotherapy.

A current limitation is that many studies including this study lack functional CMA analysis and rely instead on levels of LAMP2A or other CMA components. Although LAMP2A knockdown by RNAi-based therapeutics may be a novel therapeutic strategy for many types of cancer, LAMP2A is a difficult target owing to its high homology with other splice variants of the *LAMP2A* gene that are involved in other cellular processes. Therefore, we need to develop the method to monitor CMA status and generate selective inhibitors of CMA in humans for cancer treatment. We propose that tumor-specific dysregulation of CMA may be considered as a novel

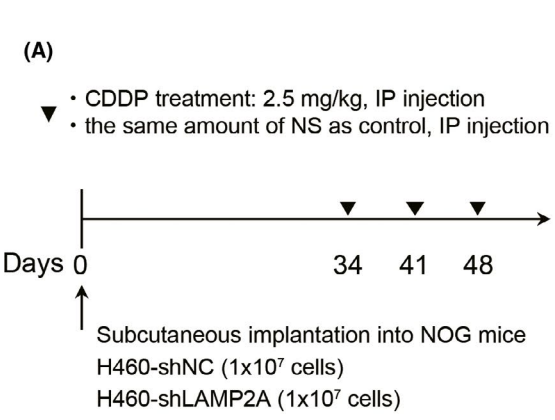
(A)
• CDDP treatment: 2.5 mg/kg, IP injection
• the same amount of NS as control, IP injection
Days 0
34
41
48
Subcutaneous implantation into NOG mice
H460-shNC (1x10⁷ cells)
H460-shLAMP2A (1x10⁷ cells)

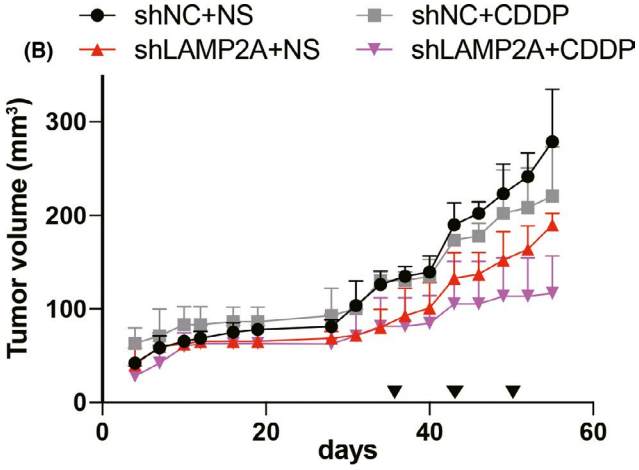
(B)
shNC+NS
shNC+CDDP
shLAMP2A+NS
shLAMP2A+CDDP
Tumor volume (mm³)
300
200
100
0
0
20
40
60
days

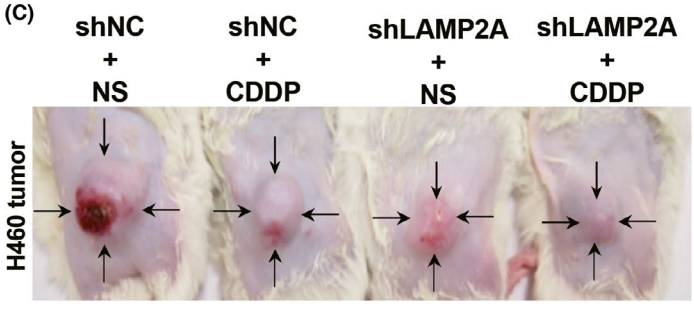
(C)
shNC + NS
shNC + CDDP
shLAMP2A + NS
shLAMP2A + CDDP
H460 tumor

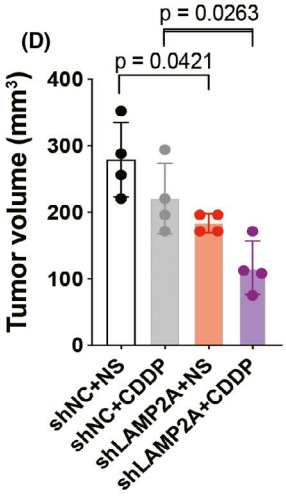
(D)
p = 0.0263
p = 0.0421
Tumor volume (mm³)
400
300
200
100
0
shNC+NS
shNC+CDDP
shLAMP2A+NS
shLAMP2A+CDDP

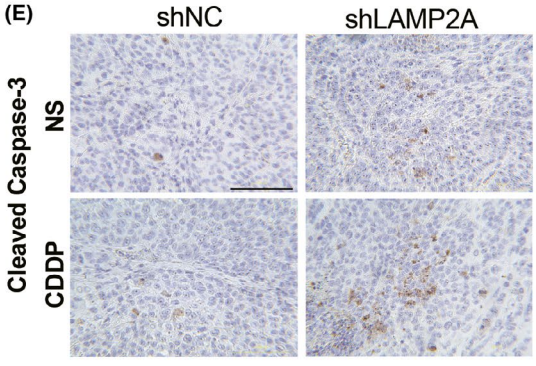
(E)
shNC
shLAMP2A
Cleaved Caspase-3
NS
CDDP

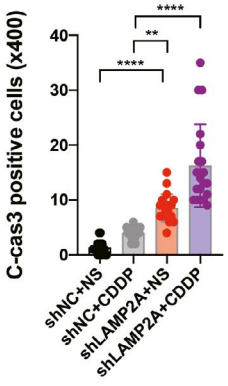
C-cas3 positive cells (x400)
****
**
****
40
30
20
10
0
shNC+NS
shNC+CDDP
shLAMP2A+NS
shLAMP2A+CDDP

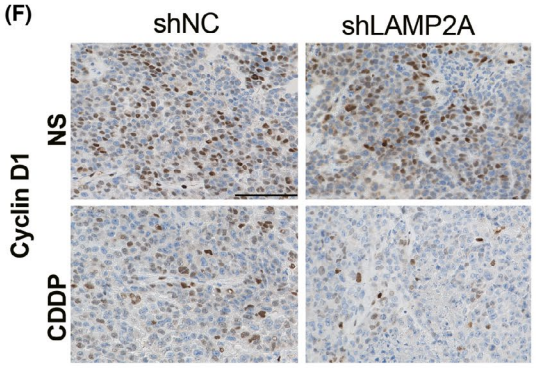
(F)
shNC
shLAMP2A
Cyclin D1
NS
CDDP

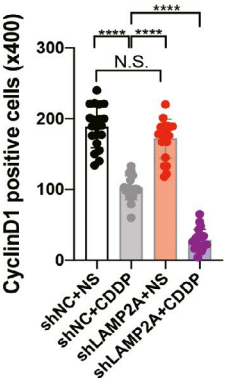
CyclinD1 positive cells (x400)
****
****
****
N.S.
300
200
100
0
shNC+NS
shNC+CDDP
shLAMP2A+NS
shLAMP2A+CDDP

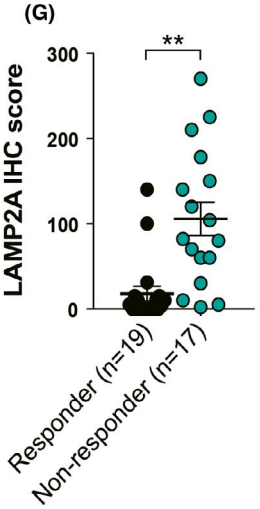
(G)
**
LAMP2A IHC score
300
200
100
0
Responder (n=19)
Non-responder (n=17)

FIGURE 4 LAMP2A regulates drug resistance and survival in vivo. A, The protocol of the repeat intraperitoneal (IP) injection of cisplatin (CDDP) or the same amount of normal saline (NS) into NOD/Shi-scid, IL-2RγKO Jic mice (NOG) mice. B, Tumor volume in H460-shNC and H460-shLAMP2A treated with CDDP or NS (each group n = 4). The treatment was performed on days 34, 41, and 48 (▼; once a week for 3 weeks, three treatment total) after subcutaneous implantation of 1×10^7 cells into NOG mice. C, Representative pictures of subcutaneous tumors (indicated by arrows) and (D) tumor volume of H460-shNC and -shLAMP2A cells treated with CDDP or NS at 56 days after subcutaneous implantation of the cells. *P*-value by ANOVA and Bonferroni's post-test. IHC staining for (E) cleaved caspase-3 and (F) cyclin D1 in the tumors of H460-shNC and -shLAMP2A cells treated with CDDP or NS (scale bar 100 μm). $^{**}P < .01$ $^{****}P < .0001$, by ANOVA and Bonferroni's post-test. G, LAMP2A IHC score in the responder (n = 19) and nonresponder group (n = 17) to platinum-based chemotherapy (Table S2) in the cohort. $^{**}P < .001$, by Student's *t*-test

therapeutic strategy for inducing tumor apoptosis and chemosensitivity in NSCLC.

In summary, we showed that LAMP2A expression correlated with responses of NSCLC patients to platinum-based chemotherapy. Analysis of clinical samples in our study demonstrated that LAMP2A was highly expressed in nonresponders compared with the responders of NSCLC patients to platinum-based chemotherapy. A complete understanding of the precise function of LAMP2A in NSCLC may allow for the use of LAMP2A as a biomarker for predicting patient response to platinum-based chemotherapy, further assisting in the development of new therapeutic strategies.

ACKNOWLEDGEMENT

This work was supported, in part, by grants from the Japan Society for the Promotion of Science KAKENHI (JP17K09672, JP17K09673, JP17K09674, JP18K08158, JP19K17649, JP19K08612, and JP19K08632). The National Cancer Center Biobank is supported by the National Cancer Center Research and Development Fund, Japan. We gratefully thank Shuichi Watanabe (Department of Thoracic Surgery, National Cancer Center Hospital, Tokyo, Japan) for providing clinical samples and Misato Yamamoto for excellent technical assistance.

CONFLICT OF INTEREST

The authors declare that no conflict of interest exists with regard to this study.

AUTHOR CONTRIBUTIONS

YF conceived the idea and coordinated the project. A. Ichikawa and YF performed the experimental work, and YF wrote the draft of the manuscript. YH, TK, A. Ito, SY, NW, HK, NS, MY, MH, SM, HH, NM, and YY helped with the experimental work and data analysis. TO, JA, and KK provided helpful discussion. The manuscript was finalized by YF with the assistance of all authors.

ORCID

Yu Fujita https://orcid.org/0000-0002-8916-7303
Noriko Motoi https://orcid.org/0000-0001-7098-3311
Yusuke Yamamoto https://orcid.org/0000-0002-5262-8479
Takahiro Ochiya https://orcid.org/0000-0002-0776-9918

REFERENCES

1. Chen T, Chen L. Prediction of clinical outcome for all stages and multiple cell types of non-small cell lung cancer in five countries using lung cancer prognostic index. *EBioMedicine*. 2014;1:156-166.
2. Mizushima N, Komatsu M. Autophagy: renovation of cells and tissues. *Cell*. 2011;147:728-741.
3. Mizushima N, Levine B, Cuervo AM, Klionsky DJ. Autophagy fights disease through cellular self-digestion. *Nature*. 2008;451:1069-1075.
4. Shpilka T, Elazar Z. Shedding light on mammalian microautophagy. *Dev Cell*. 2011;20:1-2.
5. Kaushik S, Cuervo AM. The coming of age of chaperone-mediated autophagy. *Nat Rev Mol Cell Biol*. 2018;19:365-381.
6. Kon M, Kiffin R, Koga H, et al. Chaperone-mediated autophagy is required for tumor growth. *Sci Transl Med*. 2011;3(109):109ra117.
7. Zhou J, Yang J, Fan X, et al. Chaperone-mediated autophagy regulates proliferation by targeting RND3 in gastric cancer. *Autophagy*. 2016;12:515-528.
8. Vakifahmetoglu-Norberg H, Kim M, Xia HG, et al. Chaperone-mediated autophagy degrades mutant p53. *Genes Dev*. 2013;27:1718-1730.
9. Ali AB, Nin DS, Tam J, Khan M. Role of chaperone mediated autophagy (CMA) in the degradation of misfolded N-CoR protein in non-small cell lung cancer (NSCLC) cells. *PLoS One*. 2011;6:e25268.
10. Arias E, Cuervo AM. Pros and cons of chaperone-mediated autophagy in cancer biology. *Trends Endocrinol Metab*. 2020;31:53-66.
11. Ohmori T, Morikage T, Sugimoto Y, et al. The mechanism of the difference in cellular uptake of platinum derivatives in non-small cell lung cancer cell line (PC-14) and its cisplatin-resistant subline (PC-14/CDDP]. *Jpn J Cancer Res*. 1993;84:83-92.
12. Fujita Y, Khateb A, Li Y, et al. Regulation of S100A8 stability by RNF5 in intestinal epithelial cells determines intestinal inflammation and severity of colitis. *Cell Rep*. 2018;24:3296-3311 e3296.
13. Fujita Y, Yagishita S, Hagiwara K, et al. The clinical relevance of the miR-197/CKS1B/STAT3-mediated PD-L1 network in chemoresistant non-small-cell lung cancer. *Mol Ther*. 2015;23:717-727.
14. Furuta K, Ikeda M, Nakayama Y, et al. Expression of lysosome-associated membrane proteins in human colorectal neoplasms and inflammatory diseases. *Am J Pathol*. 2001;159:449-455.
15. Saha T. LAMP2A overexpression in breast tumors promotes cancer cell survival via chaperone-mediated autophagy. *Autophagy*. 2012;8:1643-1656.
16. Okayama H, Kohno T, Ishii Y, et al. Identification of genes upregulated in ALK-positive and EGFR/KRAS/ALK-negative lung adenocarcinomas. *Cancer Res*. 2012;72:100-111.
17. Aniento F, Roche E, Cuervo AM, Knecht E. Uptake and degradation of glyceraldehyde-3-phosphate dehydrogenase by rat liver lysosomes. *J Biol Chem*. 1993;268:10463-10470.
18. Dice JF. Peptide sequences that target cytosolic proteins for lysosomal proteolysis. *Trends Biochem Sci*. 1990;15:305-309.
19. Guo B, Li L, Guo J, et al. M2 tumor-associated macrophages produce interleukin-17 to suppress oxaliplatin-induced apoptosis in hepatocellular carcinoma. *Oncotarget*. 2017;8:44465-44476.
20. Wu JH, Guo JP, Shi J, et al. CMA down-regulates p53 expression through degradation of HMGB1 protein to inhibit irradiation-triggered apoptosis in hepatocellular carcinoma. *World J Gastroenterol*. 2017;23:2308-2317.

21. Du C, Huang D, Peng Y, et al. 5-Fluorouracil targets histone acetyltransferases p300/CBP in the treatment of colorectal cancer. *Cancer Lett*. 2017;400:183-193.

SUPPORTING INFORMATION

Additional supporting information may be found online in the Supporting Information section.

How to cite this article: Ichikawa A, Fujita Y, Hosaka Y, et al. Chaperone-mediated autophagy receptor modulates tumor growth and chemoresistance in non–small cell lung cancer. *Cancer Sci*. 2020;111:4154–4165. https://doi.org/10.1111/cas.14629